

## Supporting Information

### Radiolabeling and Preclinical Evaluation of A new S-alkylated Cysteine Derivative conjugated to C-substituted Macrocycle for Positron Emission Tomography

*Surbhi Prakash<sup>†</sup>, Puja Panwar Hazari<sup>\*†</sup>, Virendra Kumar Meena<sup>†</sup>, Anil Kumar Mishra<sup>\*†</sup>*

<sup>†</sup>Division of Cyclotron and Radiopharmaceutical Sciences, Institute of Nuclear Medicine and Allied Sciences, Brig SK Mazumdar Road, Delhi-110054, India. Email: akmishra63@gmail.com

<b>Figure S1</b> <sup>1</sup> H NMR spectrum of di-tert-butyl 2,2'-(12-amino-11,13-dioxo-1,4,7,10-tetraazacyclotridecane-4,7-diyl)diacetate( <b>2</b> )	S3
<b>Figure S2</b> <sup>13</sup> C NMR spectrum of di-tert-butyl 2,2'-(12-amino-11,13-dioxo-1,4,7,10-tetraazacyclotridecane-4,7-diyl)diacetate( <b>2</b> )	S3
<b>Figure S3</b> LC-MS mass spectrum of di-tert-butyl 2,2'-(12-amino-11,13-dioxo-1,4,7,10-tetraazacyclotridecane-4,7-diyl)diacetate( <b>2</b> )	S4
<b>Figure S4</b> HRMS spectrum of di-tert-butyl 2,2'-(12-amino-11,13-dioxo-1,4,7,10-tetraazacyclotridecane-4,7-diyl)diacetate( <b>2</b> )	S4
<b>Figure S5</b> <sup>1</sup> H NMR spectrum of di-tert-butyl 2,2'-(12-(2-chloroacetamido)-11,13-dioxo-1,4,7,10-tetraazacyclotidecane-4,7-diyl)diacetate( <b>3</b> )	S5
<b>Figure S6</b> <sup>13</sup> C NMR spectrum of di-tert-butyl 2,2'-(12-(2-chloroacetamido)-11,13-dioxo-1,4,7,10-tetraazacyclotidecane-4,7-diyl)diacetate( <b>3</b> )	S5
<b>Figure S7</b> LC-MS spectrum of di-tert-butyl 2,2'-(12-(2-chloroacetamido)-11,13-dioxo-1,4,7,10-tetraazacyclotidecane-4,7-diyl)diacetate( <b>3</b> )	S6
<b>Figure. S8</b> HRMS spectrum of di-tert-butyl 2,2'-(12-(2-chloroacetamido)-11,13-dioxo-1,4,7,10-tetraazacyclotidecane-4,7-diyl)diacetate( <b>3</b> )	S6
<b>Figure. S9</b> <sup>1</sup> H NMR spectrum of 2-acetamido-3-((2-((4,7-bis(2-(tert-butoxy)-2-oxoethyl)-11,13-dioxo-1,4,7,10-tetraazacyclotidecan-12-yl)amino)-2-oxoethyl)thio)propanoic acid( <b>4</b> )	S7
<b>Figure. S10</b> <sup>13</sup> C NMR spectrum of 2-acetamido-3-((2-((4,7-bis(2-(tert-butoxy)-2-oxoethyl)-11,13-dioxo-1,4,7,10-tetraazacyclotidecan-12-yl)amino)-2-oxoethyl)thio)propanoic acid( <b>4</b> )	S7
<b>Figure. S11</b> LC-MS spectrum of 2-acetamido-3-((2-((4,7-bis(2-(tert-butoxy)-2-oxoethyl)-11,13-dioxo-1,4,7,10-tetraazacyclotidecan-12-yl)amino)-2-oxoethyl)thio)propanoic acid( <b>4</b> )	S8
<b>Figure. S12</b> HRMS spectrum of 2-acetamido-3-((2-((4,7-bis(2-(tert-butoxy)-2-oxoethyl)-11,13-dioxo-1,4,7,10-tetraazacyclotidecan-12-yl)amino)-2-oxoethyl)thio)propanoic acid( <b>4</b> )	S8

<b>Figure S13</b> $^1\text{H}$ NMR spectrum of 2,2'-(12-(2-((2-acetamido-2-carboxyethyl)thio)acetamido)-11,13-dioxo-1,4,7,10-tetraazacyclotidecane-4,7-diyl)diacetic acid ( <b>5</b> )	S9
<b>Figure S14</b> $^{13}\text{C}$ NMR spectrum of 2,2'-(12-(2-((2-acetamido-2-carboxyethyl)thio)acetamido)-11,13-dioxo-1,4,7,10-tetraazacyclotidecane-4,7-diyl)diacetic acid ( <b>5</b> )	S9
<b>Figure S15</b> LC-MS Spectrum of 2,2'-(12-(2-((2-acetamido-2-carboxyethyl)thio)acetamido)-11,13-dioxo-1,4,7,10-tetraazacyclotidecane-4,7-diyl)diacetic acid ( <b>5</b> )	S10
<b>Figure S16</b> HRMS spectrum of 2,2'-(12-(2-((2-acetamido-2-carboxyethyl)thio)acetamido)-11,13-dioxo-1,4,7,10-tetraazacyclotidecane-4,7-diyl)diacetic acid ( <b>5</b> )	S10
<b>Figure S17</b> HPLC profile of Ga-ATRIDAT-NAC at 230 nm.	S11
<b>Figure S18</b> Radio-tlc scan of [ $^{68}\text{Ga}$ -ATRIDAT-NAC] before and after cartridge purification from ez-tlc scanner	S11
<b>Figure S19</b> Optimization of Radiolabeling with respect to heating time, pH, and precursor concentration used and temperature.	S12
<b>Figure S20</b> Graph showing clearance of radiolabeled compound from the blood of female Wistar rat with time injected intravenously.	S13
<b>Figure S21</b> Graph showing stability of radiolabeled compound in human serum	S13

**Figure S1**  $^1\text{H}$ NMR spectrum of di-tert-butyl 2,2'-(12-amino-11,13-dioxo-1,4,7,10-tetraazacyclotridecane-4,7-diyl)diacetate(2)

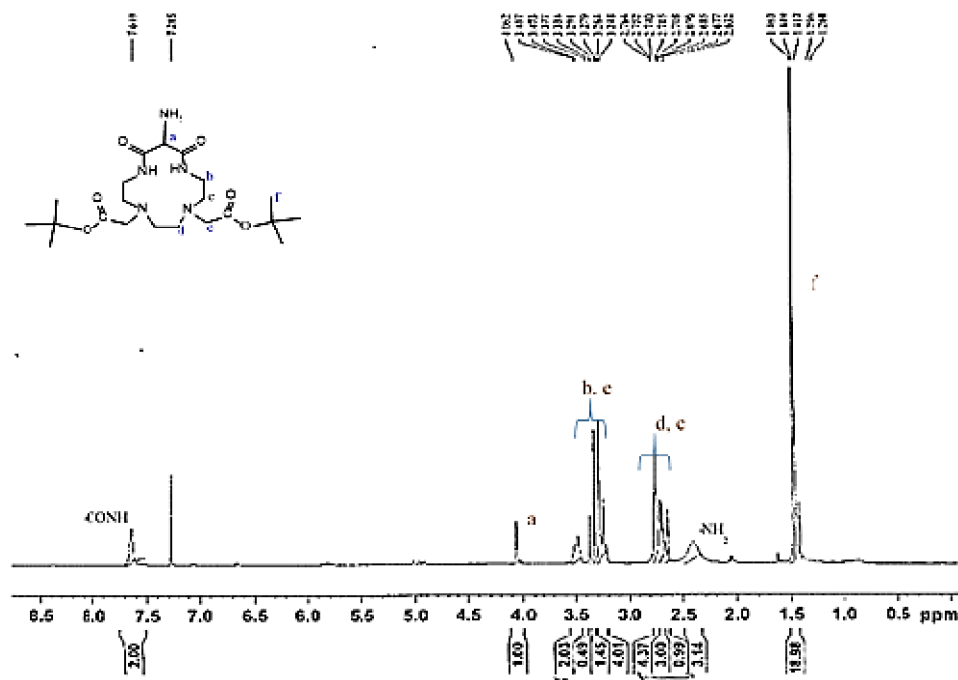


**Figure S2**  $^{13}\text{C}$ NMR spectrum of di-tert-butyl 2,2'-(12-amino-11,13-dioxo-1,4,7,10-tetraazacyclotridecane-4,7-diyl)diacetate(2)

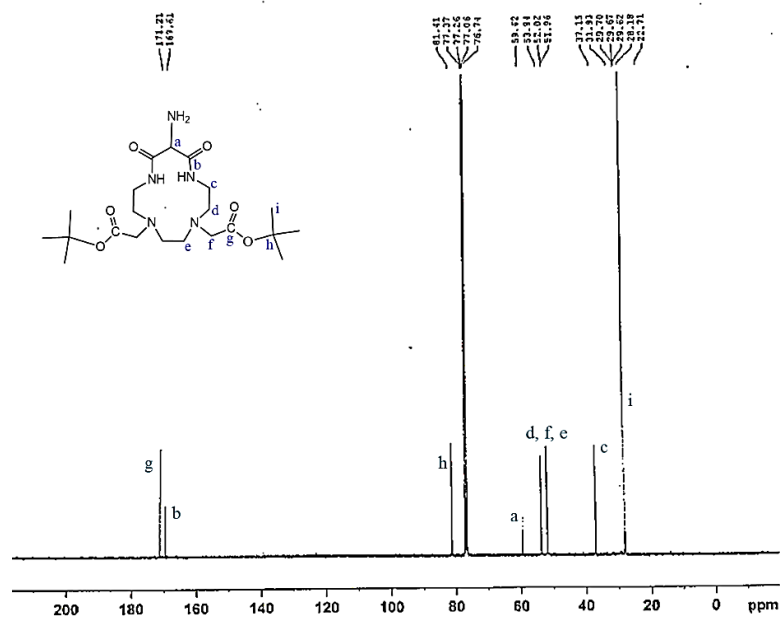


**Figure S3LC-MS** mass spectrum of di-tert-butyl 2,2'-(12-amino-11,13-dioxo-1,4,7,10-tetraazacyclotridecane-4,7-diyl)diacetate(2)

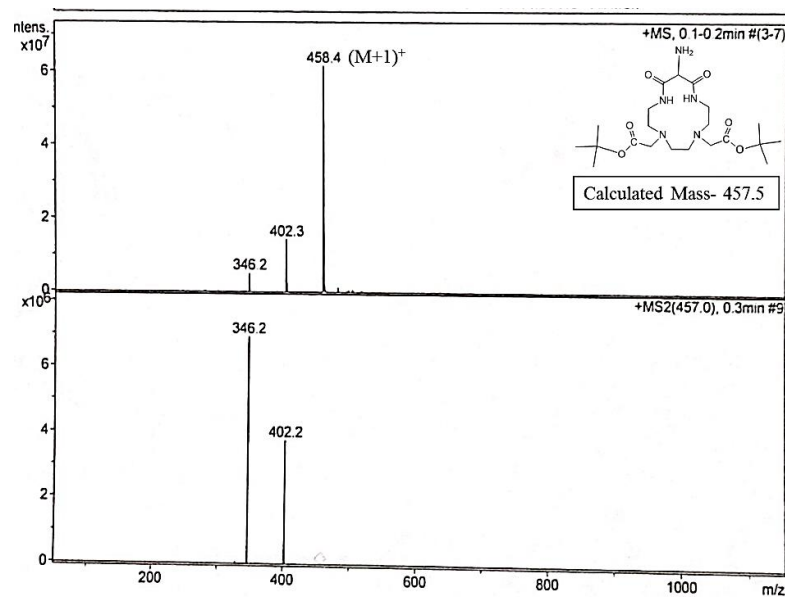


**Figure S4** HRMS spectrum of di-tert-butyl 2,2'-(12-amino-11,13-dioxo-1,4,7,10-tetraazacyclotridecane-4,7-diyl)diacetate(2)

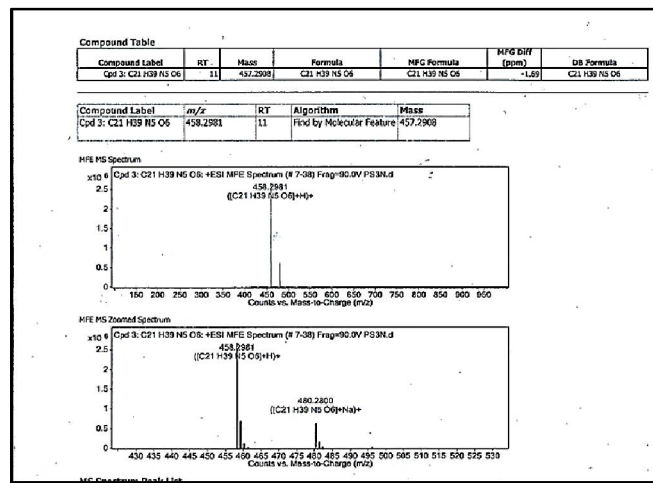


**Figure S5**  $^1\text{H}$ NMR spectrum of di-tert-butyl2,2'-(12-(2-chloroacetamido)-11,13-dioxo-1,4,7,10-tetraazacyclotridecane-4,7-diyl)diacetate(3)

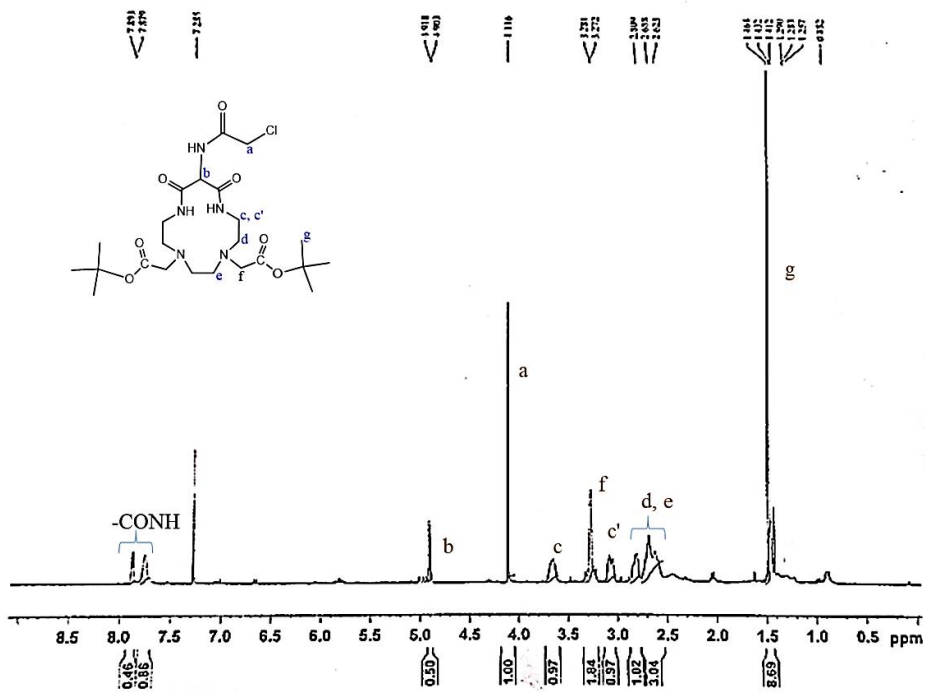


**Figure S6**  $^{13}\text{C}$ NMR spectrum of di-tert-butyl2,2'-(12-(2-chloroacetamido)-11,13-dioxo-1,4,7,10-tetraazacyclotridecane-4,7-diyl)diacetate(3)

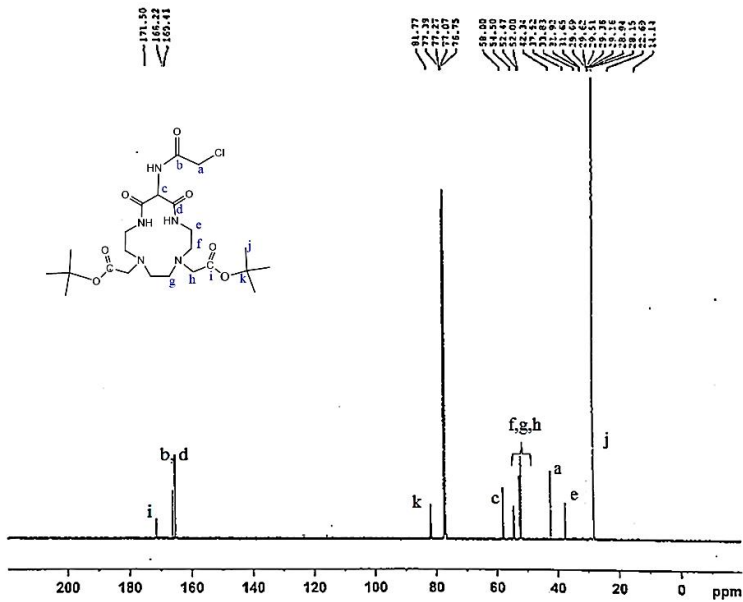


**Figure S7** LC-MS spectrum of di-tert-butyl 2,2'-(12-(2-chloroacetamido)-11,13-dioxo-1,4,7,10-tetraazacyclotridecane-4,7-diyl)diacetate(**3**)

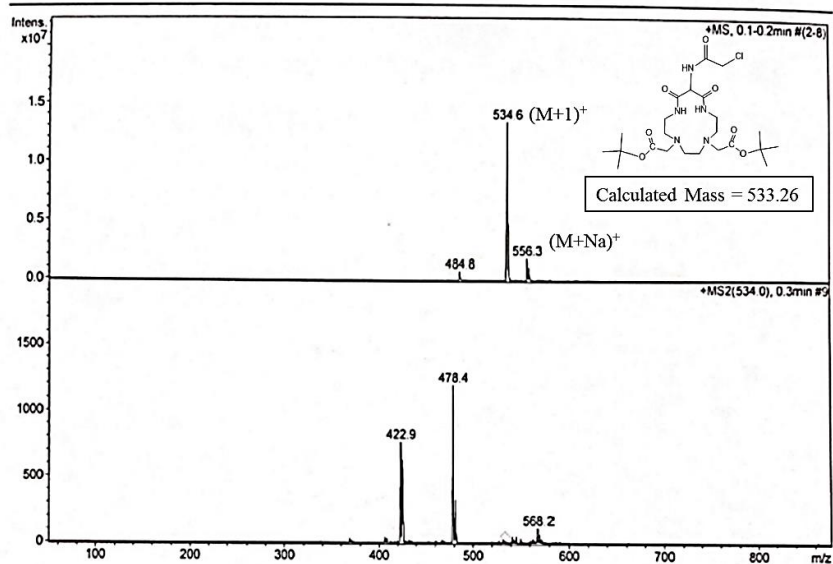


**Figure S8** HRMS spectrum of di-tert-butyl 2,2'-(12-(2-chloroacetamido)-11,13-dioxo-1,4,7,10-tetraazacyclotridecane-4,7-diyl)diacetate(**3**)

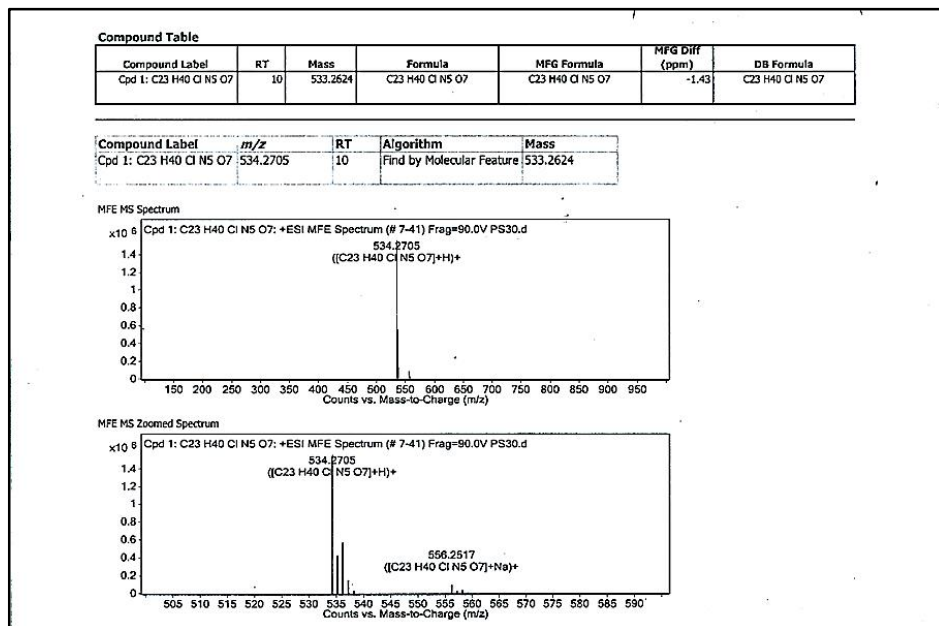


**Figure S9**  $^1\text{H}$ NMR spectrum of 2-acetamido-3-((2-((4,7-bis(2-(tert-butoxy)-2-oxoethyl)-11,13-dioxo-1,4,7,10-tetraazacyclotridecan-12-yl)amino)-2-oxoethyl)thio)propanoic acid(**4**)

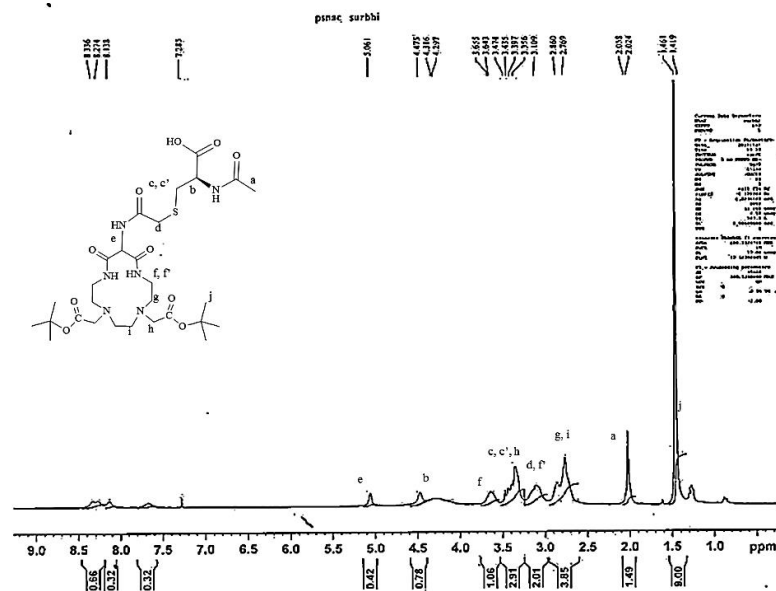


**Figure S10**  $^{13}\text{C}$ NMR spectrum of 2-acetamido-3-((2-((4,7-bis(2-(tert-butoxy)-2-oxoethyl)-11,13-dioxo-1,4,7,10-tetraazacyclotridecan-12-yl)amino)-2-oxoethyl)thio)propanoic acid(**4**)

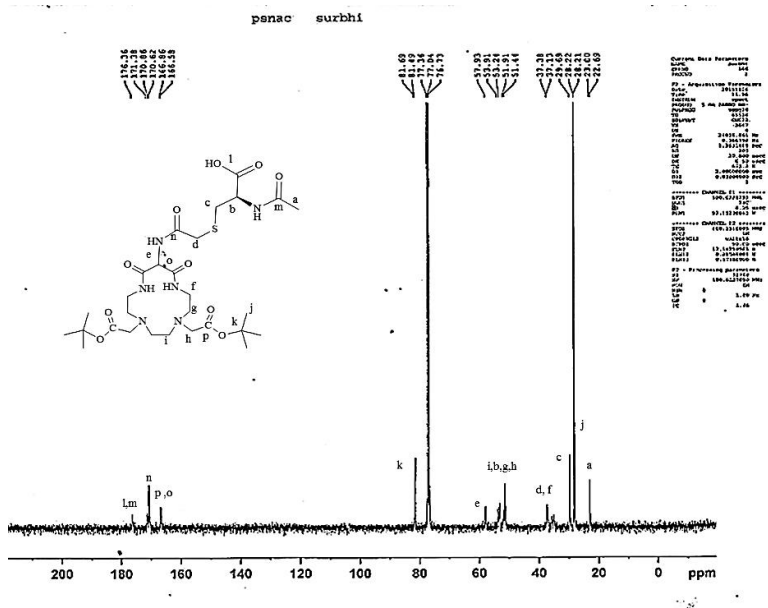


**Figure S11** LC-MS spectrum of 2-acetamido-3-((2-((4,7-bis(2-(tert-butoxy)-2-oxoethyl)-11,13-dioxo-1,4,7,10-tetraazacyclotridecan-12-yl)amino)-2-oxoethyl)thio)propanoic acid(**4**)

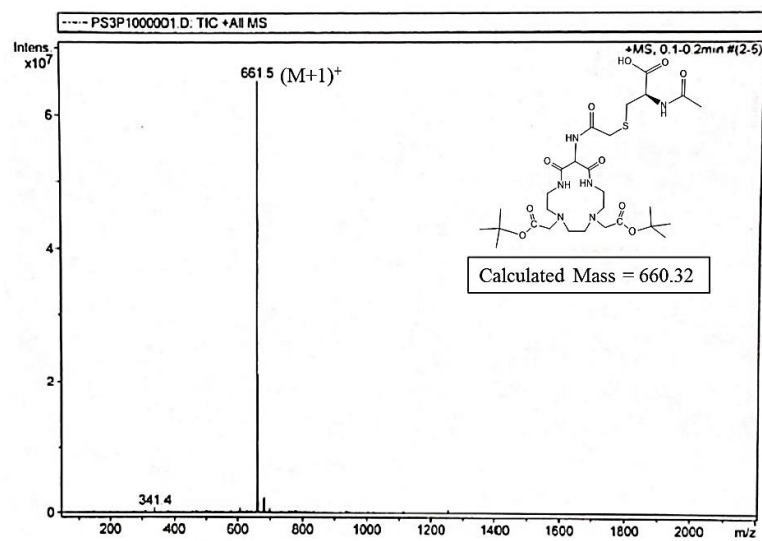


**Figure S12** HRMS spectrum of 2-acetamido-3-((2-((4,7-bis(2-(tert-butoxy)-2-oxoethyl)-11,13-dioxo-1,4,7,10-tetraazacyclotidecan-12-yl)amino)-2-oxoethyl)thio)propanoic acid(**4**)

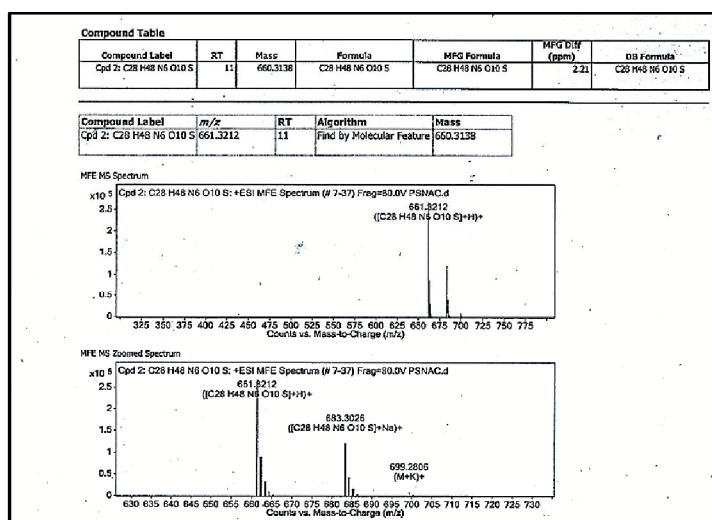


**Figure S13**  $^1\text{H}$ NMR spectrum of 2,2'-(12-(2-((2-acetamido-2-carboxyethyl)thio)acetamido)-11,13-dioxo-1,4,7,10-tetraazacyclotridecane-4,7-diyl)diacetic acid (**5**)

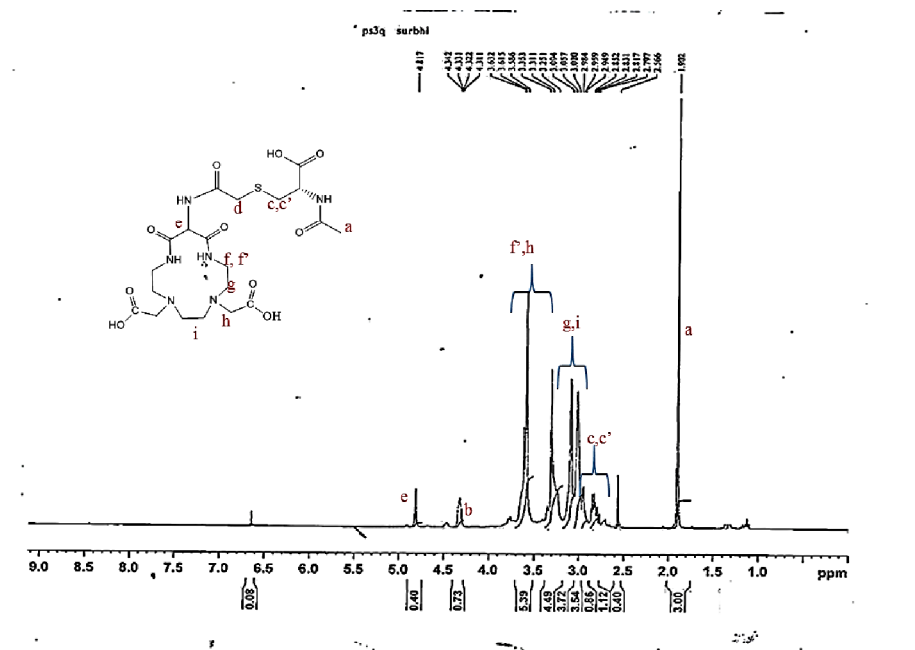


**Figure S14**  $^{13}\text{C}$ NMR spectrum of 2,2'-(12-(2-((2-acetamido-2-carboxyethyl)thio)acetamido)-11,13-dioxo-1,4,7,10-tetraazacyclotridecane-4,7-diyl)diacetic acid (**5**)

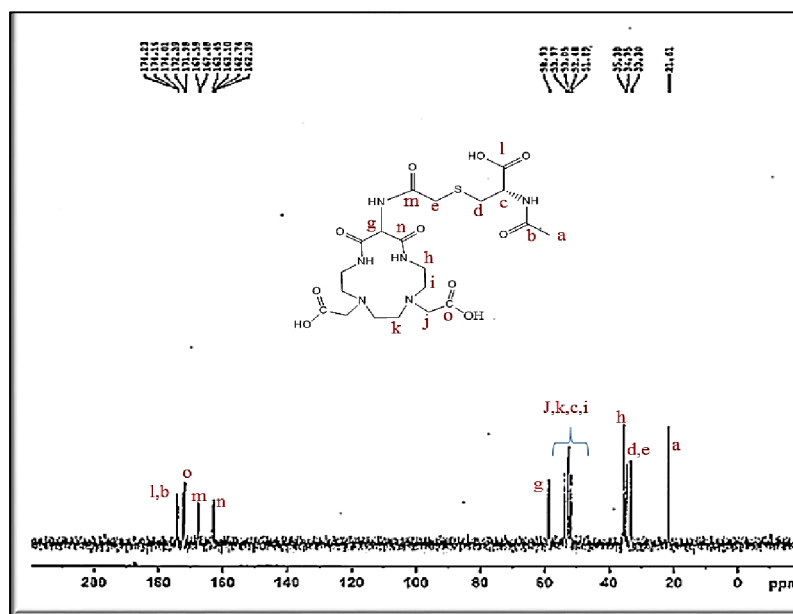


**Figure S15** LC-MS spectrum of 2,2'-(12-(2-((2-acetamido-2-carboxyethyl)thio)acetamido)-11,13-dioxo-1,4,7,10-tetraazacyclotridecane-4,7-diyl)diacetic acid (**5**)

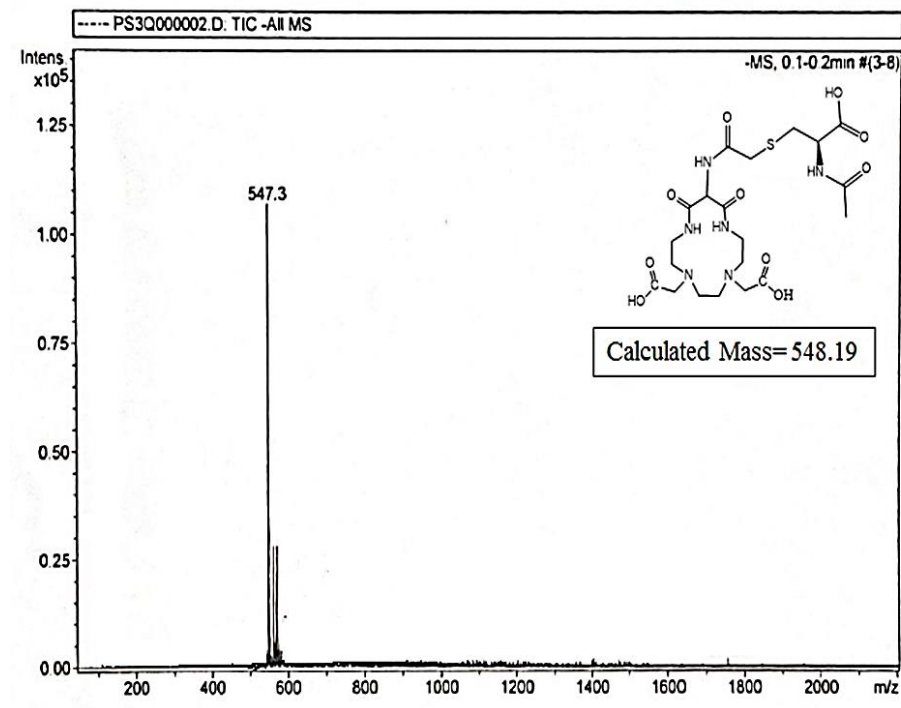


**Figure S16** HRMS spectrum of 2,2'-(12-(2-((2-acetamido-2-carboxyethyl)thio)acetamido)-11,13-dioxo-1,4,7,10-tetraazacyclotridecane-4,7-diyl)diacetic acid (**5**)

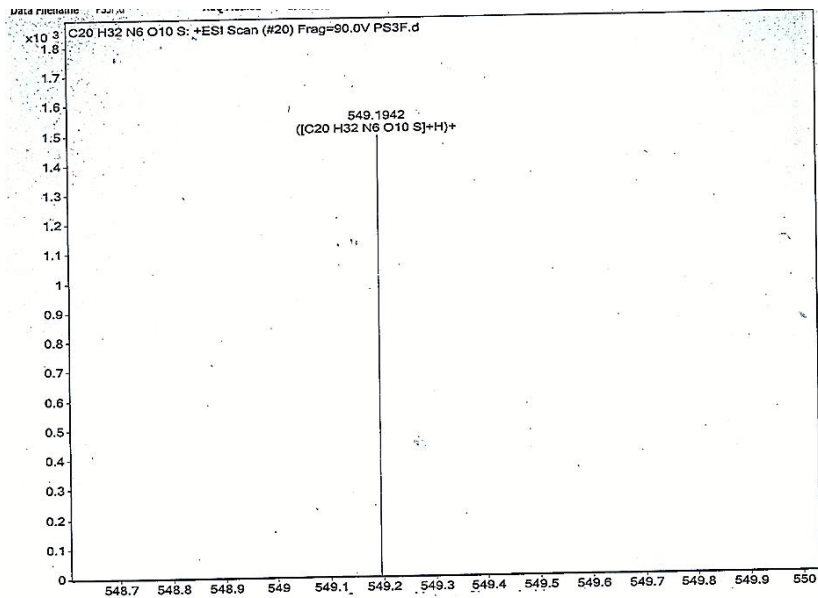


**Figure S17** HPLC profile of Ga-ATRIDAT-NAC at 230 nm.

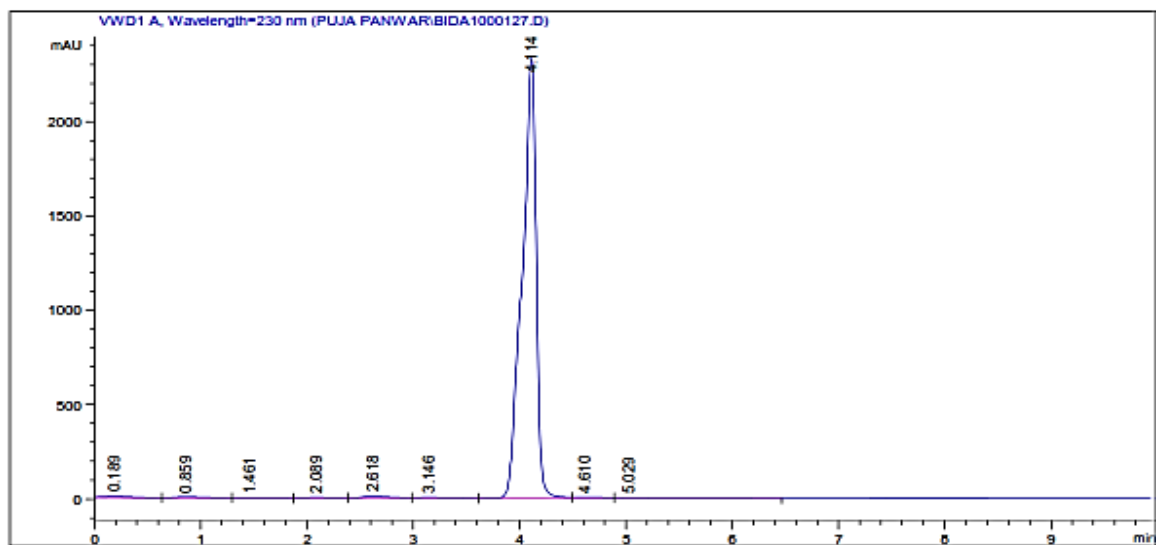
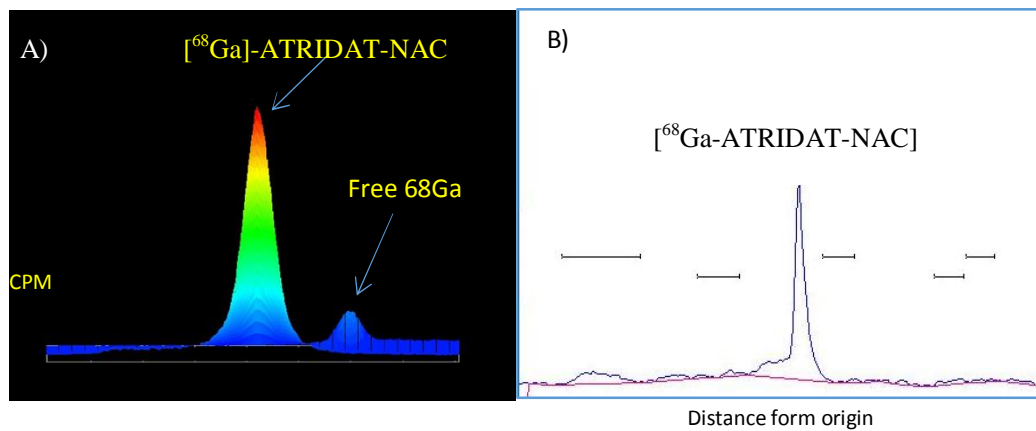
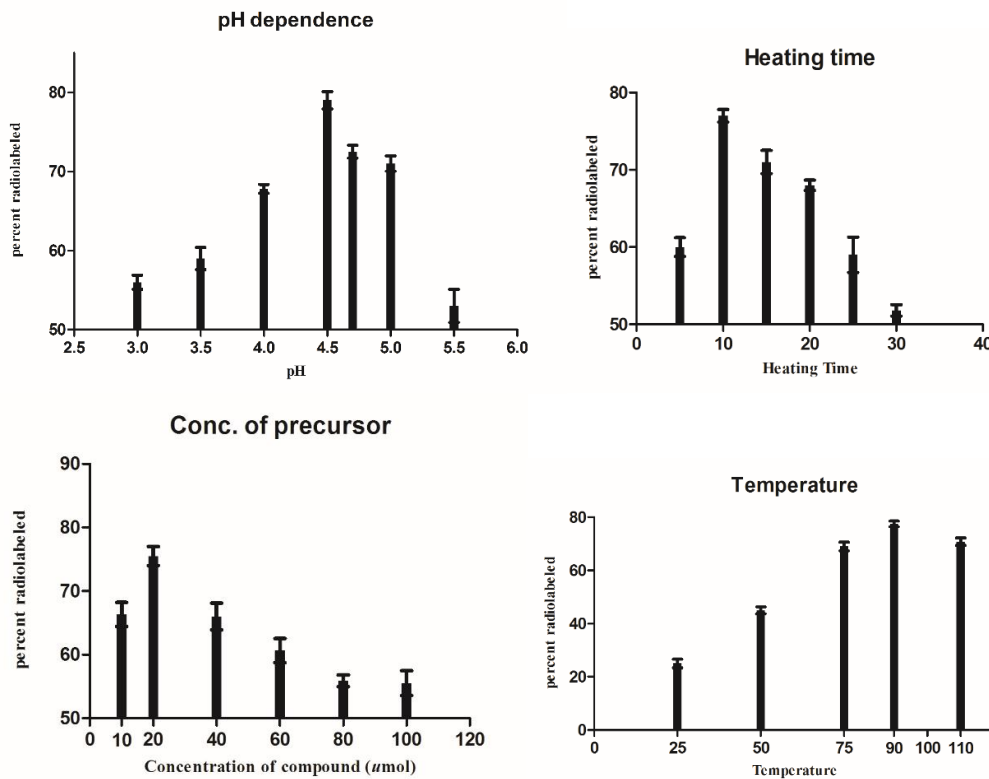


**Figure S18** Radio-tlc scan of [ $^{68}\text{Ga}$ -ATRIDAT-NAC] from ez-tlc scanner



**A)** Before cartridge purification **B)** After cartridge purification [ $^{68}\text{Ga}$ -ATRIDAT-NAC] peak

**Figure S19** Optimization of Radiolabeling with respect to heating time, pH, and precursor concentration used and temperature.



When pH was changed from 3 to 4.5, the activity increased from 56 to 79 % and then further decreased to 53 % on further increasing the pH to 5.5. When radiolabeling was performed at room temperature, 25 % radiolabeling was achieved which increased to 77.5 % at 90 °C and did not increase on further increasing the temperature. Best radiolabeling yield was obtained by heating for 10 min. On further heating, the radiolabeling yield got reduced to nearly 50 %. 20  $\mu\text{mol}$  concentration of radiolabeled compound gave highest radiolabeling yield of 75.5 % which decreased on further increasing the concentration.

**Figure S20** Graph showing clearance of radiolabeled compound from the blood of female Wistar rat with time injected intravenously.

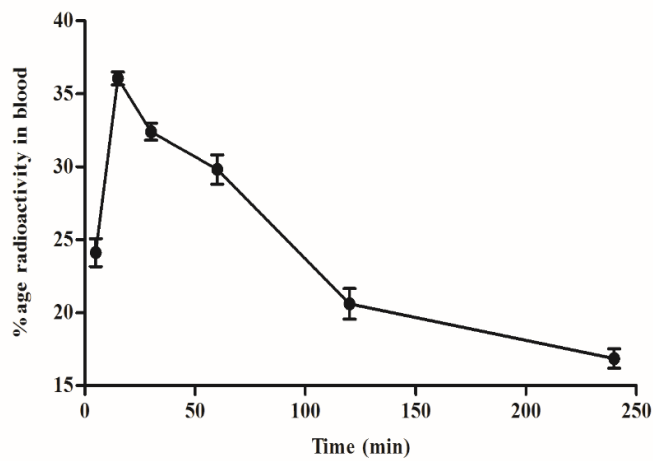


**Figure S21** Graph showing stability of radiolabeled compound in human serum

